



HAL
open science

Unravelling solvent response to neutral and charged solutes

Maxim V Fedorov, Alexei A. Kornyshev

► **To cite this version:**

Maxim V Fedorov, Alexei A. Kornyshev. Unravelling solvent response to neutral and charged solutes. Molecular Physics, 2007, 105 (01), pp.1-16. 10.1080/00268970601110316 . hal-00513060

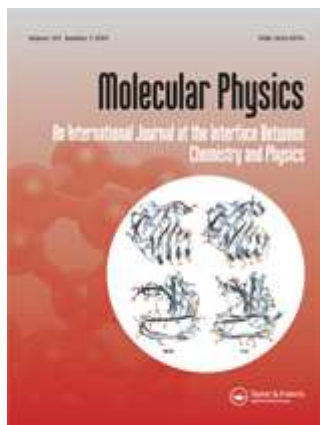
HAL Id: hal-00513060

<https://hal.science/hal-00513060>

Submitted on 1 Sep 2010

HAL is a multi-disciplinary open access archive for the deposit and dissemination of scientific research documents, whether they are published or not. The documents may come from teaching and research institutions in France or abroad, or from public or private research centers.

L'archive ouverte pluridisciplinaire **HAL**, est destinée au dépôt et à la diffusion de documents scientifiques de niveau recherche, publiés ou non, émanant des établissements d'enseignement et de recherche français ou étrangers, des laboratoires publics ou privés.



Unravelling solvent response to neutral and charged solutes

Journal:	<i>Molecular Physics</i>
Manuscript ID:	TMPH-2006-0022
Manuscript Type:	Invited Article
Date Submitted by the Author:	15-Sep-2006
Complete List of Authors:	Fedorov, Maxim; University of Cambridge, Chemistry Kornyshev, Alexei; Imperial College London, Chemistry
Keywords:	ion hydration, integral equations , nonlocal electrostatics, statistical mechanics, theory of liquids



Unravelling solvent response to neutral and charged solutes

Maxim V. Fedorov* and Alexei A. Kornyshev†

* Unilever Centre for Molecular Science Informatics, Department of Chemistry, University of Cambridge, Lensfield Road, CB2 1EW Cambridge, UK

† Department of Chemistry, Faculty of Natural Sciences, Imperial College London, SW7 2AZ London, UK

(Received 00 Month 200x; In final form 00 Month 200x)

In this article we discuss the effects of solute-water interactions with a focus on a set of old standing questions:

- How strong is the nonlinear response of water polarisation to charged solute?
- How strong is the asymmetry of the response between cations and anions of similar size?
- What is the role of the finite size of the solute?
- How 'positive' or 'negative' hydration manifests itself in the dielectric response?
- Can nonlocal electrostatics, based on the bulk value of solvent dielectric function, be used to describe the electric field of an ion and its hydration?
- Are experimental data on hydration energies compatible with the hypothesis of over-screening effect in the bulk solvent response?

The answers rest on a crude but analytically viable model of water (modified SPC/E); in no way final, they are intended to provoke future more sophisticated studies, based on *ab initio* quantum molecular dynamic simulations and new experiments.

1 Introduction

The studies of ionic solvation (hydration, in particular) have more than a hundred year history and many achievements [1–3]. Various aspects of solvation have been reviewed in 80s in a comprehensive three volume collective monograph [4–6]. One of the central questions put forward there has been, 'what is the role of the solvent structure in the solvent response to a charged solute?'. The following two decades were characterised by intensive development of new methods for the description of the solvent, based on computer simulations [7–18] and the approximate statistical mechanics of molecular liquids [19–26], as well as further exploration of the semi-phenomenological approach which describes the solvent via the nonlocal

* Corresponding author. Email: mvf22@cam.ac.uk

† Email: a.kornyshev@imperial.ac.uk

2

1 dielectric function [27–31]. The latter was a successor of the classical Born and Debye theories (in which
2 the solvent is described through its macroscopic dielectric constant). But in contrast to those theories,
3 'nonlocal electrostatics' does not operate with a dielectric constant, but with nonlocal dielectric function,
4 which in turn can be expressed through the pair correlation function of bound charge density fluctuations of
5 the polar liquid or electrolyte in the bulk. For given form-factors of charge distributions inside the solvent
6 molecule or electrolyte ions, this correlation function is related to the atomic partial structure factors
7 (static, when fluctuations are classical, i.e. have frequencies smaller than k_B/\hbar , or dynamic, otherwise).
8 For more about these concepts see, e.g., in Ref. [13].

9 There were two main obstacles against using nonlocal electrostatics:

- 10 • The form of the nonlocal dielectric function in polar solvent, water in particular, remained to be a
11 subject of debates, and depended strongly on the model of the liquid.
- 12 • It was not clear how much the presence of the solute perturbs the surrounding liquid, and whether it
13 was possible at all to incorporate the nonlocal dielectric function of the bulk water into the description
14 of ionic solvation, as some approximations suggested [29, 31].

15 The 'primary suspects' for such disturbances were:

- 16 • Nonlinear response of the solvent to the field of the ion, known under the notion of dielectric saturation.
- 17 • Physical distortion of the short range structure of the solvent by the finite size of the solute.
- 18 • Specific solute-solvent interaction, including covalent or hydrogen bonding.

19 The latter may be present or not, but the first two factors cannot be ignored a priori. The first one is
20 charge dependent, and is stronger the greater the charge. Although there were some interesting results
21 showing at which field-strength the dielectric saturation becomes significant [32–35], there was no consensus
22 about the critical value of charge which sets a boundary between the linear and nonlinear response. As
23 this should clearly depend on the size of the solute (near small ions the electric field is larger), how
24 large must the ion charge and ion size be for dielectric saturation to take place? Pioneer simulations by
25 Geiger [36] illuminated micro-dynamics of water around the ion of variable charge and size, but their effect
26 on equilibrium structures has not been quantified.

27 The second factor distorts the structure sterically if the ion does not fit hypothetical 'voids' in the water
28 hydrogen bonded network.

29 These issues are concerned with the Samoilov's notions of 'positive' and 'negative' hydration [1, 37],
30 and even hydrophobic hydration [38], but the questions that we want to revisit are: 'how these structural

1 changes caused by the solute affect the overall solvent dielectric response, hydration energies, the form of
2 electric field around the solute, etc?'

3
4 Although each of these points has been raised in some form before, in this article we wish to analyse them
5 systematically on the basis of one approach. We will use an integral equation scheme – Reference Interaction
6 Site Model (RISM) [39], which provides an approximate statistical-mechanical description of the solute-
7 solvent interactions based on a rigid model of water. Specifically, it will be the MSPC/E model [40], a
8 slightly modified version of the well-known SPC/E model [41]. Obviously, *this water is not 'drinkable'*: the
9 molecular model is not accurate, nor is the integral equation closure exact. But the reason for this exercise
10 was to get answers to these questions in *one calculation* within the *same model*, which would have been
11 difficult within computationally much more demanding MD simulations. Additional advantages of this
12 approach are the exact reproducibility of calculations, and the ease with which the values of parameters
13 and conditions may be changed.
14
15

16 Will the answers that we obtain be true for real water?
17

18 We do not expect any *conceptual* changes from employing other methods of classical statistical me-
19 chanics, at least as long as the charge distribution in water molecule is described by rigid point charges.
20 But the analysis, presented in Ref. [42] shows that just smearing of charge distributions between oxygen
21 and hydrogen in the spirit of the Bader and Jones model [43] changes results a lot! Generally, classical
22 statistical mechanics models with point charges cannot describe such important effects as: *charge transfer*
23 and *electronic polarisability*. Although, these models simulate hydrogen bonding, but in a very crude fash-
24 ion. So, real changes can be expected improving on this front. Modern force-fields [44, 45] and polarisable
25 water models [46–48] may be helpful but they ordinary invoke additional empirical parameters, targeted
26 not to ideally describe water itself, but rather to compare the 'performance' of this water in different
27 environments. An example of this is the proton transfer model of Ref. [47], used for the analysis of the
28 effect of charged pore walls on the proton transfer in polymer electrolyte membranes [49] (for discussion
29 see Ref. [50]).
30
31

32 Future ab initio quantum-mechanical MD simulations will be the best fit to answer this question. With
33 modern terascale computers and state-of-the-art numerical methods [51], such simulations will soon become
34 a reality. The questions and answers presented in this Article could provoke and help to focus these future
35 studies. Its second goal is to get a flavour of several qualitative effects that come out from the model.
36 Throughout the paper we will compare 'our answers' with those obtained in the literature for similar
37 models.
38
39
40
41
42
43
44
45
46
47
48
49
50
51
52
53
54
55
56
57
58
59
60

2 Theoretical methods.

Recent theoretical and computational developments have made it possible to describe different solvation phenomena with good accuracy. The most popular (and the most accurate) methods of classical statistical mechanics are the methods of direct simulation of solute-solvent systems such as Monte-Carlo and Molecular Dynamics. Due to the progress in computer science and numerical methods of quantum mechanics, the *first principle* molecular simulations of solvation effects seem to be also possible. Such simulation methods are very useful for understanding fundamental properties of solute-solvent interactions, but they require huge computational resources. Even in the case of 'unlimited' access to modern supercomputers and use of advanced numerical methods [51] the *ab initio* simulations are still limited by the size of the simulation ensemble ($\lesssim 1000$ atoms) and simulation time ($\lesssim 1000$ ps) [52–54]. With such limitations it is difficult to evaluate *macroscopic* parameters, such as the dielectric susceptibility.

An alternative to Molecular Mechanic simulations is the integral equations (IE) theory [55–57]. Although approximate, the results have been shown to be meaningful for pure liquids and different solutions [21, 23, 24, 58–64]. Despite the apparent limitations, IE theory has a number of advantages over molecular simulation: for small solutes it is much faster than any MD or MC simulation, the solutions are free of statistical noise and the thermodynamic limit is by definition attained, thus avoiding numerical artifacts due to the finite-size simulation cell. In this way, phenomena related to large correlation lengths become accessible. Another advantage of IE theories is that the free energy and chemical potential in the case of the hypernetted chain (HNC) approximation [65] or its analogues [66, 67] are directly related to the correlation functions. It has been shown that IE-HNC theory is able to describe different properties of polar fluids with a reasonable degree of accuracy [19–21].

At present there are several approaches based on integral equations. The molecular Ornstein-Zernike (MOZ) theory is the method to calculate three dimensional (3D) solvation structure in molecular liquids. The MOZ theory treats the orientation dependence of intermolecular interactions through the rotational invariant expansions of interaction potentials and correlation functions [68].

Another approach is the RISM formalism. This model was first developed by Chandler and Andersen [39] and then modified by different authors to describe properties of complex solute-solvent systems (ex-RISM or XRISM) [20, 21]. The theory is based on calculations of radial distribution functions (RDF) via the site-site Ornstein-Zernike (SSOZ) integral equation. This model provides detailed information about solute-solvent interactions in terms of statistically averaged site-site distribution functions. The theory has been successfully applied to calculate the structural and thermodynamic properties of various chemical

1 and biological systems [55, 57]. In Ref. [20] the HNC closure was employed to consider the nonlinear
2 response of solvent. One of the drawbacks of this approach is the fact, that the numerical procedure can
3 become divergent in the case of strong solute-solvent interactions. Kovalenko and Hirata [66, 67] proposed
4 a partial linearisation of the HNC closure (PLHNC) to eliminate this artifact. In the both RISM-HNC
5 and RISM-PLHNC approaches the solvation free energy can be expressed as a function of the RDFs and
6 the direct correlation functions (see more details below in the subsections (2.3) and (2.4)). It was shown
7 that the RISM-HNC(PLHNC) approximation provides an appropriate description of liquids containing
8 polar solutes [19–21]. However, this model strongly overestimates the energy of hydrogen bonding. As a
9 consequence, this method provides poor predictions for the thermodynamics of hydrophobic solvation. To
10 improve the theory, an orientational average of the Boltzmann factor for a repulsive core potential of the
11 whole solvent molecule has been incorporated in the 3D RISM/HNC closure [69]. Kovalenko and Hirata
12 extended this repulsive bridge correction (RBC) to the 'one dimensional' (1D) RISM approach [66, 67].
13 In this study we use the 1D RISM/PLHNC model improved by the RBC for the case of hydrated ionic
14 species [70]. We employ this model to calculate thermodynamic and structural properties of hydrated
15 model solutes.
16
17
18
19
20
21
22
23
24
25
26
27
28

29 We use below the Lue and Blankshtein version of SPC/E model of water [41] referred to as the modified
30 SPC/E model (MSPC/E) [40, 71]. The modification includes a weak Lennard-Jones potential between
31 the water oxygens and hydrogens, totally neglected in the original SPC/E model. The SPC/E water
32 itself is common because in spite of its simplicity it reproduces the most significant features of water at
33 room temperature such as the internal energy, pressure, and RDFs [41]. For calculation of water radial
34 correlation functions we used a reformulation of RISM with dielectric corrections [22, 72, 73] to provide
35 accurate screening of the long-range interactions. The details of these methods and parameters of the
36 model are described in the Appendix.
37
38
39
40
41
42
43

44 For the purposes of this study it was sufficient to consider a system composed of a single monatomic
45 (spherically symmetric) solute with radius a in aqueous solvent.
46
47
48
49
50
51
52
53

54 2.1 *Linear Response Formalism*

56 The classical form of the fluctuation-dissipation theorem (FDT) connects the longitudinal component of
57 the wave vector dependent static dielectric tensor with the structural properties of the bulk medium in
58
59
60

the following way [8]:

$$\epsilon(k) = \left[1 - \frac{4\pi S(k)}{k_B T} \right], \quad (1)$$

where $S(k) = \langle \rho_{\mathbf{k}} \rho_{-\mathbf{k}} \rangle / k^2$ is the charge density structure factor ($\rho_{\mathbf{k}}$ is the Fourier transform of the bound charge density).

$S(k)$ may be found from the partial density structure factors $g_{ij}(k) = \langle n_{i,\mathbf{k}} n_{j,-\mathbf{k}} \rangle / N$ of the charged sites i and j (oxygen and hydrogen for water) which may be obtained either from scattering experiments or some theoretical calculations. If we separate the intramolecular (m) and intermolecular (d) contributions to $S(k) = S^m(k) + S^d(k)$ we may write for bulk water:

$$S^m(k) = \frac{2nz^2e^2}{k^2} \left[3 + f_{HH}(k) \frac{\sin(kd_{HH})}{kd_{HH}} - 4f_{OH}(k) \frac{\sin(kd_{OH})}{kd_{OH}} \right]; \quad (2)$$

$$S^d(k) = \frac{4nz^2e^2}{k^2} [g_{OO}(k) + g_{HH}(k) - 2g_{OH}(k)] \quad (3)$$

$$= \frac{4nz^2e^2}{k^2} \int_0^\infty 4\pi r^2 \frac{\sin(kr)}{kr} [g_{OO}(r) + g_{HH}(r) - 2g_{OH}(r)] dr, \quad (4)$$

where n is molecular number density of the fluid; z , the valence; e , the electron charge, g_{ij} are the site-site pair density correlation functions, and d_{ij} , the mean intramolecular distances. The f_{ij} are distribution functions which characterise the equilibrium fluctuations of the site-site distances from their mean values, thereby including atomic form factors. For rigid molecules with point charges on the sites, $f_{ij}(k) = 1$. This is the case for the MSPC/E water model which we are using in this work.

Within the framework of linear nonlocal electrostatics and the so-called *immersed charge approximation* (in which the ion is represented by a charge distribution which does not structurally perturb but only polarises the surrounding solvent), the form of electrostatic potential around the ion with a spherical charge distribution $\rho(r)$ is completely determined by the properties of $\epsilon(k)$ [4, 30, 74] and by the Fourier transform of the ion charge density:

$$\rho(k) = \int_0^\infty 4\pi \frac{\sin(kr)}{(kr)} \rho(r) r^2 dr. \quad (5)$$

The expression for the potential reads

$$\Phi^{nonlocal}(r) = \frac{2}{\pi} \int_0^\infty \frac{\rho(k)}{\epsilon(k)} \frac{\sin(kr)}{(kr)} dk. \quad (6)$$

The most common approximations for the ion charge density is the **Born Sphere** model (BS) [4], for which

$$\rho_{BS}(k) = q \frac{\sin(ka)}{ka}. \quad (7)$$

For the **Smeared Born Sphere** model (SBS) [30]:

$$\rho_{SBS}(k) = \frac{q}{1 + (\xi/a)^2 (2 - e^{-a/\xi})} \left(\frac{\sin(ka)}{ka} \frac{1}{1 + \xi^2 k^2} + \frac{\xi^2 (2\cos(ka) - e^{-a/\xi})}{a^2 (1 + \xi^2 k^2)^2} \right). \quad (8)$$

The BS model assumes that the charge is uniformly distributed over a sphere of radius a (the ion radius). In the SBS model, the charge density has a maximum at the radial distance a from the centre of the sphere; from this distance it decreases exponentially (both outside and inside the sphere) with decay length ξ . In the limit of $\xi \rightarrow 0$, the SBS model reduces to the BS model.

With the use of the immerse charge approximation, the free energy of ion hydration ΔG is calculated via equation [30]:

$$\Delta G = \frac{1}{\pi} \int_0^\infty \rho(k)^2 \left[1 - \frac{1}{\epsilon(k)} \right] dk. \quad (9)$$

For the **Born Sphere** model of an ion it is known as the Dogonadze-Kornyshev equation [27] which describes well the hydration energies of alkali and halide ions under the assumption of Lorentzian behaviour of the dielectric function [29]. But it had difficulties to reconcile the presence of the overscreening peak in $[1 - \frac{1}{\epsilon(k)}]$ that can be, however, relaxed by introduction of the SBS model [30].

2.2 Electrostatic Potential around a spherical solute in molecular liquid

A spherically symmetric monatomic solute immersed in a molecular solvent creates electrostatic potential which can be represented as a sum of two terms: $\Phi(r) = \Phi^c(r) + \Phi^*(r)$. Here $\Phi^c(r)$ is the Coulomb potential in vacuum $\Phi^c(r) = q_I/r$ (q_I is the electrostatic charge of the solute) and $\Phi^*(r)$ is an induced electrostatic

potential due to the polarisation response of solvent molecules to the presence of the solute. $\Phi^*(r)$ can be written in terms of the spherically symmetric ion-solvent RDFs g_{Is} as [24]:

$$\Phi^*(r) = 4\pi\rho_v \left[\frac{1}{r} \sum_s q_s \int_0^r g_{Is}(r')r'^2 dr' + \sum_s q_s \int_r^\infty g_{Is}(r')r' dr' \right], \quad (10)$$

where ρ_v is the density of the solvent and q_s is the charge of a solvent site s . We used this formula in all our calculations of $\Phi(r)$.

Generally, since all our examples will refer only to spherically symmetric solutes and, thereby, to spherically symmetric solvent polarisation and perturbations of the solvent structure around the solute, we will be able to reduce the problem to the radial parts of the corresponding correlation functions. This would not be the case if we had tried to establish how the presence of the solute perturbs the pattern of the *binary correlation functions* near the solvent. The latter would have been the most direct and unambiguous information about the solute effect on the solvent structure. Unfortunately, this is difficult to achieve within the present method of analysis, and we leave this challenging task for the future studies.

2.3 RISM Integral Equation Theory for Molecular Liquids

The main elements of this theory have been well described in the literature (see e.g. Ref. [57]). However, for the sake of completeness, we briefly outline them. The RISM integral equation theory, as developed by Chandler and Andersen [39], consists of integral equations with two different kinds of unknown functions, the total correlation functions, $h(\mathbf{r}) = g(\mathbf{r}) - 1$, and the direct correlation functions, $c(\mathbf{r})$, where \mathbf{r} is the distance variable and $g(\mathbf{r})$ is the density correlation function.

Let us determine the convolution product $x(\mathbf{r}) * y(\mathbf{r})$ of two functions $x(\mathbf{r})$ and $y(\mathbf{r})$ as:

$$x(\mathbf{r}) * y(\mathbf{r}) = \int x(|\mathbf{r} - \mathbf{r}'|)y(\mathbf{r}')d\mathbf{r}'. \quad (11)$$

In the following we assume all the correlation functions are spherically symmetric, and depend only on the distance from the centre of the corresponding site $r = |\mathbf{r}|$.

Let us also introduce an intramolecular correlation function:

$$\omega_{ij} = \delta_{ij}\delta(r) + \varpi_{ij}(r), \quad (12)$$

where δ is the Kronecker symbol, function $\varpi_{ij}(r)$ describes the position of sites i and j within a single molecule. For a rigid molecule it is given by

$$\varpi_{ij} = \frac{(1 - \delta_{ij}) \delta(r - L_{ij})}{(4\pi L_{ij}^2)}, \quad (13)$$

where the L_{ij} is the distance between the sites i and j .

The extended RISM integral equations (XRISM) for a system that consists of a molecular solvent and a solute at infinite dilution could be written as [57]:

$$h_{\alpha\beta}^{vv}(r) = \sum_{\gamma,\zeta} \omega_{\alpha\gamma}^v(r) * c_{\gamma\zeta}^{vv}(r) * (\omega_{\zeta\beta}^v(r) + \rho_v h_{\zeta\beta}^{vv}(r)), \quad (14)$$

and

$$h_{s\alpha}^{uv}(r) = \sum_{s',\gamma} \omega_{ss'}^u(r) * c_{s'\gamma}^{uv}(r) * (\omega_{\gamma\alpha}^v(r) + \rho_v h_{\gamma\alpha}^{vv}(r)), \quad (15)$$

where ρ_v is the average solvent density, the superscripts v and u correspond to the solvent and the solute, Latin symbols denote the solute sites and Greek symbols denote the solvent sites.

To find a solution of the Eqns. (14) and (15) one has to complete them by a closure relation which connects h – and c – functions with the same combination of 'v' and 'u' indices in a local way as [57]:

$$h_{ij}(r) = \exp(-\beta u_{ij}(r) + h_{ij}(r) - c_{ij}(r) + B_{ij}(r)) - 1. \quad (16)$$

Here, $B_{ij}(r)$ is a bridge function, $u_{ij}(r)$ is a spherically symmetric pair potential between interaction sites i and j , symbol β denotes the inverse temperature: $\beta = (k_B T)^{-1}$, where k_B is the Boltzmann constant and T is the absolute temperature. The case $B(r) \equiv 0$ corresponds to the the Hypernetted Chain closure (HNC) closure. The Partially Linearised Hypernetted Chain closure [66,67] linearises the exponent in (16) for the case of $B(r) \equiv 0$ depending on the sign of the function $\Xi_{ij}(r) = -\beta u_{ij}(r) + h_{ij}(r) - c_{ij}(r)$:

$$c_{ij}(r) = \begin{cases} \exp(\Xi_{ij}(r)) - h_{ij}(r) + c_{ij}(r) - 1 & \Xi_{ij}(r) < 0 \\ -\beta u_{ij}(r) & \Xi_{ij}(r) > 0 \end{cases} \quad (17)$$

10

1 In this model the site-site interaction potential $u_{ij}(r)$ consists of a short-ranged potential $u_{ij}^*(r)$ and a long
 2 range Coulomb potential $u_{ij}^c(r) = q_i q_j / r_{ij}$, where q_i and q_j are the partial charges of the interaction sites
 3 i and j . In this work we use standard Lennard–Jones (LJ) short range potential:
 4
 5
 6
 7

$$8 \quad u_{ij}^*(r) = 4\eta_{ij} \left(\left[\frac{\sigma_{ij}}{r} \right]^{12} - \left[\frac{\sigma_{ij}}{r} \right]^6 \right). \quad (18)$$

9
 10
 11 The site-site LJ parameters σ_{ij} and η_{ij} are determined according to the standard Lorentz-Berthelot com-
 12 bining rule: [56]:
 13
 14

$$15 \quad \sigma_{ij} = \frac{1}{2}(\sigma_i + \sigma_j), \quad \eta_{ij} = (\eta_i \eta_j)^{\frac{1}{2}}. \quad (19)$$

16
 17 Such details of the RISM technique as dielectric corrections and numerical treatment of the long-range
 18 electrostatic interactions are described in the Appendix.
 19
 20
 21

22 2.4 RISM Solvation Free Energy and Repulsive Bridge Correction

23
 24 Within the scope of RISM-HNC theory the thermodynamic functions of solvation can be described in terms
 25 of the correlation functions given above. The excess RISM-HNC chemical potential $-\beta\Delta\mu^{HNC}$ (solvation
 26 free energy) of a **monatomic ion** (I) at infinite dilution has the form [75]:
 27
 28

$$29 \quad -\beta\Delta\mu^{HNC} = 4\pi\rho_v \sum_{\alpha} \int_0^{\infty} \left\{ \frac{1}{2}h_{I\alpha}(r)^2 - c_{I\alpha}(r) - \frac{1}{2}h_{I\alpha}(r)c_{I\alpha}(r) \right\} r^2 dr, \quad (20)$$

30 where α refers to the interaction sites of solvent molecules. The PLHNC gives similar expression for
 31 chemical potential [67]:
 32
 33
 34

$$35 \quad -\beta\Delta\mu^{PLHNC} = 4\pi\rho_v \sum_{\alpha} \int_0^{\infty} \left\{ \frac{1}{2}h_{I\alpha}(r)^2 \Theta(-h_{I\alpha}(r)) - c_{I\alpha}(r) - \frac{1}{2}h_{I\alpha}(r)c_{I\alpha}(r) \right\} r^2 dr, \quad (21)$$

36 where $\Theta(x)$ is the Heaviside step function.
 37
 38

39 In the RISM model we can express the total energy of ion-solvent interactions H_I via the ion-solvent
 40 radial correlations functions as:
 41
 42
 43
 44

$$45 \quad H_I = 4\pi\rho_v \sum_{\alpha} \int_0^{\infty} [1 + h_{I\alpha}(r)] u_{I\alpha}(r) r^2 dr. \quad (22)$$

Therefore, in the case of non-zero bridge function $B(r)$ (see Eq. (16)), one can use more general Kirkwood formula [76] to calculate the hydration free energy:

$$\Delta\mu = \int_0^1 \left\langle \frac{\partial H_I(r, \lambda)}{\partial \lambda} \right\rangle_{\lambda} d\lambda = 4\pi\rho_v \sum_{I\alpha} \int_0^1 d\lambda \int_0^{\infty} [1 + h_{I\alpha}(r, \lambda)] \left\langle \frac{\partial u_{I\alpha}(r, \lambda)}{\partial \lambda} \right\rangle_{\lambda} r^2 dr. \quad (23)$$

where λ is a coupling parameter which is determined on the interval 0 (unhydrated ion) to 1 (fully hydrated ion). This relation requires calculation of ion-solvent correlation functions $h_{I\alpha}(r, \lambda)$ at different values of λ .

There is a common practice to use two *different* coupling parameters λ_{nel} and λ_{el} for *separate* calculations of the nonpolar $\Delta\mu_{nel}$ and the electrostatic $\Delta\mu_{el}$ free energy contributions, respectively [77]. If the interaction potential $u_{I\alpha}$ has the form (18) the 'nonpolar' λ_{nel} is considered as a scaling factor of the LJ radius σ_{Ij} , i.e. $\sigma_{Ij}(\lambda_{nel}) = \lambda_{nel}\sigma_{I\alpha}$. Similarly, the coupling parameter λ_{el} is considered as a scaling factor of the solute charge, $q_I(\lambda_{el}) = \lambda_{el}q_I$. Therefore, we may express $\Delta\mu$ as:

$$\Delta\mu = \Delta\mu_{nel} + \Delta\mu_{el}, \quad \Delta\mu_{el} = \int_0^1 \left\langle \frac{\partial H_I^{el}(\lambda_{el})}{\partial \lambda} \right\rangle_{\lambda_{el}} d\lambda_{el}, \quad (24)$$

where H_I^{el} is the electrostatic part of the total energy H_I :

$$H_I^{el}(\lambda_{el}) = 4\pi\rho_v \sum_{\alpha} \int_0^{\infty} [1 + h_{I\alpha}(r)] \frac{\lambda_{el}q_Iq_{\alpha}}{r} r^2 dr. \quad (25)$$

In the case of water solvent the derivation $\left\langle \frac{\partial H_I^{el}(\lambda_{el})}{\partial \lambda} \right\rangle_{\lambda_{el}}$ can be expressed via the total solute-oxygen (h_{IO}) and solute-hydrogen (h_{IH}) correlation functions

$$\left\langle \frac{\partial H_I^{el}(\lambda_{el})}{\partial \lambda} \right\rangle_{\lambda_{el}} = 4\pi\rho_v q_I \int_0^{\infty} [2q_H h_{IH}(r, \lambda_{el}) - q_O h_{IO}(r, \lambda_{el})] r dr, \quad (26)$$

where ρ_v is the averaged water density, while q_H and q_O are the hydrogen and oxygen partial charges of the water molecule.

To achieve better accuracy in prediction of the nonpolar part of solvation free energy $\Delta\mu_{nel}$ than it is provided by the HNC/PLHNC theory, we use the recently developed repulsive bridge correction (RBC) technique for 1D RISM [70, 78]. In this case the bridge function has non-zero value which is determined

1 by this relation:

$$2 \exp[-B_{ij}(r)] = \prod_{l \neq j} \omega_{il}(r) * \exp[-4\beta\eta_j(\frac{\sigma_{lj}}{r})^{12}]. \quad (27)$$

3
4
5
6
7
8
9 The authors of Ref. [69] proposed such form of the bridge function for the three-dimensional (3D) orien-
10 tational reduction of the MOZ equation for a one-component molecular liquid. Kovalenko and Hirata [78]
11 proposed to take the repulsive core as a sum of the LJ terms, since the orientational average of the po-
12 tential provides a soft repulsion extending beyond the LJ repulsive core throughout the first hydration
13 shell and provides the correct dependence of the hydration chemical potential on the solute size [78]. An
14 analogous empirical bridge corrections were used in work [77] in the 3D RISM calculations of hydration of
15 organic molecules and in [70], where the solvation free energy of ionic species was calculated by a hybrid
16 'one-dimensional' (1D) RISM/QM scheme.
17

18 Instead of direct integration of the Eq.(23) by λ_{nel} , we calculate the nonelectrostatic contribution $\Delta\mu_{nel}$
19 by the perturbation scheme proposed in [78]:
20
21

$$22 \beta\Delta\mu_{nel} = \beta\Delta\mu_{nel}^{PLHNC} + 4\pi\rho_v \sum_{I\alpha} \int_0^\infty [1 + h_{I\alpha}^{PLHNC}(r)][\exp[-B_{I\alpha}(r)] - 1]r^2 dr, \quad (28)$$

23
24 where the correlation functions are taken with PLHNC closure (17), and $\Delta\mu_{nel}^{PLHNC}$ is calculated by (21).
25 The results of several previous studies [70,78,79] have shown, that such calculations are essentially simpler
26 and faster than the complete thermodynamic integration (23) but provide reasonable accuracy for the
27 nonpolar contribution $\Delta\mu_{nel}$ in hydration of hydrophobic and ionic solutes [70,78,79].
28
29
30
31
32

33 3 Results and Discussion

34 3.1 Nonlocal dielectric response of bulk water

35 The atom-atom total correlation functions $\{h_{OO}, h_{OH}, h_{HH}\}$ of bulk MSPC/E water were found nu-
36 merically by an iterative RISM technique with use of recently developed fast wavelet-based algorithms
37 [80–82]. These data are calculated for ambient conditions: temperature $T = 298 K$ and density of water
38 $\rho = 0.997 g/cm^3$. To find the values of correlation functions in the real space we used a uniform mesh
39 with 4096 knot points and step size $\delta R = 0.0278 \text{ \AA}$. High accuracy is vital in the case of highly charged
40 solutes to avoid numerical artifacts. Therefore, we run the iteration procedure until the mean Euclidian
41
42
43
44
45
46
47
48
49
50
51
52
53
54
55
56
57
58
59
60

1 distance between two adjacent iterations is less than 10^{-12} . The data obtained allowed us to calculate
 2 intermolecular $\{g_{OO}, g_{OH}, g_{HH}\}$ and intramolecular correlation functions and hence the charge density
 3 structure factor $S(k)$ (via Eqs. (2)-(4)) of the bulk water and the corresponding longitudinal dielectric
 4 susceptibility $\chi(k)$:
 5
 6
 7

$$10 \quad \chi(k) = 1 - \frac{1}{\epsilon(k)} = \frac{4\pi}{k_B T} S(k), \quad (29)$$

11 which is $\chi(k)$ is a smooth function in contrast to the $\epsilon(k)$ which may have discontinuities [8]. The results
 12 for $\chi(k)$ are displayed in Fig. 1. For the sake of comparison we put there also $\chi(k)$ obtained from the
 13 Molecular Dynamics simulations of bulk SPC/E water (see details of the simulations in the Appendix).
 14 Shapes of these functions look very similar to each other. The position of the main 'overscreening' peak
 15 at $k \approx 3\text{\AA}^{-1}$ is very close to what has been found in another MD simulations [8,13,83], and theoretical
 16 models of water [23], but as well as in Ref. [23, 83], the height of the peak is two times larger than it
 17 was found for the flexible BJH water model [84] that takes into account the internal degrees of freedom
 18 of water molecules (where the highest point is about 25) [8, 13]. Likewise, the Lorentzian behaviour at
 19 small k [8, 13, 85] is also missing, as clearly seen in the inset which shows the monotonic growth of $\chi(k)$
 20 from $k = 0$. Since, the sign of the derivative at $k \approx 0$ is known to be super-sensitive to the inaccuracy
 21 of calculation [86], the reliability of this conclusion even for the studied model is not warranted. This is
 22 the reason why we do not show in the inset the results obtained by the MD simulations - even with 1716
 23 water molecules in the box, the accuracy at low k is poor.
 24
 25
 26
 27
 28
 29
 30
 31
 32
 33
 34
 35
 36
 37
 38
 39
 40

41 **3.2 Gibbs free energies of hydration**

42 Using the RISM-RBC technique and employing Eqns. (24) and (28), we calculated the free energy of
 43 hydration of a spherical ion, ΔG , versus its radius a . For ion LJ parameters we used $\sigma_I = a$ and $\eta_I =$
 44 $6.41 \cdot 10^{-3} \text{ eV}$ ($0.25 k_B T$, $T = 298 \text{ K}$). We took LJ parameters of the water sites from the MSPC/E
 45 set of parameters of Ref. [71]. Then we calculated ion-hydrogen and ion-oxygen LJ interaction potentials
 46 following the Lorentz-Berthelot combining rules (19). To find the electrostatic part of free energy we used
 47 11 values of λ_{el} .
 48
 49
 50
 51
 52
 53
 54

55 Fig. 2 shows RISM-RBC (solid line) and MD (dashed line) [18] values of ΔG for neutral spheres. Qual-
 56 itatively, these results are in line with experimental data of analogous hydrophobic solutes: Ne (0.12 eV)
 57 and Ar (0.09 eV) [87]. Shapes of these curves are qualitatively similar, but the integral equations give
 58
 59
 60

1 higher values of ΔG for neutral spheres than MD calculations, presumably, because of the differences in
2
3 the shape of effective potentials between the solute and water sites.
4

5 The RISM-RBC results for charged spheres are shown on the top of Fig. 3. For comparison we also
6 placed there the results obtained with the classical Born model [88]: $\Delta G_{Born} = \frac{q^2}{2a} \left(1 - \frac{1}{\epsilon}\right)$.
7
8

9 On the bottom of Fig. 3 we show analogous results for the nonlocal theory calculations via the Dogonadze-
10 Kornyshev equation (9) (as discussed in the linear response section of the Computational Methods) with
11 the RISM values of the longitudinal bulk dielectric susceptibility $\chi(k)$. Correspondence to alkali-halide
12 ions is marked by Gourary and Adrian radii [89]. In both figures we also show experimental data for alkali
13 cations and halide anions taken from different sources [90–92].
14
15
16
17

18 Integral equation calculations just as analogous MD calculations in Ref. [12] give substantially different
19 hydration energies for cations and anions of similar radii - the anions are stronger hydrated. The differ-
20 ence was often attributed to a kind of anion hydrogen bonding with water molecules, but the differences
21 found in RISM-RBC model are larger than the experimental results. This is not unexpected, because this
22 model slightly overestimates the first proton radial distribution peak near the negative ion, relative to the
23 experimental values [78]. Although the data summarised by Salomon [90] are friendlier to the RISM-RBC
24 results, the scale of separation of anion and cation contributions to salt hydration energies that he used is
25 not ‘indisputable’.
26
27
28
29
30
31
32

33 The nonlocal electrostatic calculation with the **Born Sphere** model, which ignores any smearing of
34 solute charge and distortion of solvent structure by the solute, gives a huge overscreening contribution
35 to the hydration energies. This is substantially diminished by using **Smearing Born Sphere** model with a
36 smearing parameter $\xi = 0.4 \text{ \AA}$. But RISM-RBC does it better than BS not only because it involves a direct
37 contribution of short range repulsion of the immersed sphere (c.f. the Fig. 2) that reduces the hydration
38 energy, but also because the distortions of water structure by the presence of the immersed sphere and
39 its charge seemingly suppress the resonance dielectric response of the solvent. At the same time, the SBS
40 model with an appropriate smearing parameter ξ can also give satisfactory results for solvation free energy
41 for reasonable ionic radii ($a > 1.00 \text{ \AA}$). These results are in line with the conclusions of Refs. [63, 70, 93]
42 that hydration free energy of medium size ionic solutes are mainly determined by the structural properties
43 of bulk water and the geometry of solutes. Formally, the results of QM/MM calculations in Ref. [70] failed
44 for ion radii smaller than 1 \AA .
45
46
47
48
49
50
51
52
53
54

55 By its nature, neither Born nor its nonlocal electrostatic modification can distinguish the difference
56 between the cations and anions of the similar size, unless we fiddle with the value of parameter λ .
57
58
59
60

3.3 *Uncharged soft hydrophobic sphere*

The first feature to study here was the electric field around an *uncharged* hydrophobic sphere immersed in water. The values of these fields calculated within the MSPC/E water model are given in Fig. 4 for a set of sphere radii: 0.5, 1.0, 2.0 and 5.0 Å. The distances are measured from the surface of the sphere. It is remarkable that *an inert neutral sphere creates a short range electric field around itself*. This conclusion is in good correspondence with the results obtained by others with the use of different computational techniques. For instance, Refs [9, 12, 15, 18, 94, 95], although not having displayed distributions of electric potential, have shown nonuniform bound-charge density profiles around inert neutral spheres; nonzero fields were found in recent MD simulations, performed for a similar kind of water model [96], as well as in Ref. [97].

This effect is due to a distortion of the structure of water near the ion and consequent preferential orientation of water molecules near the surface of the sphere. Their orientation affects polarisation of water further away from the sphere at distances of short range order in the liquid. Specifically, for all radii of the spheres studied the presence of the sphere orients water molecules almost parallel to the surface (as can be seen from the water oxygen and hydrogen density profiles on the inset to Fig. 4 but with protons slightly closer to the surface, which creates an excess of the positive charge near the sphere. Large spheres cause smaller fields, since their role in the preferential orientation of water is smaller.

The corrugation of potential is a consequence of the decaying density oscillations around the sphere. On the inset to the Fig. 4 we show the density profiles for oxygen and hydrogen atoms around the neutral solutes of two sizes, with sphere radii $a = 1.0$ Å and $a = 5.0$ Å. We compared these results with those obtained in Ref. [18] from Molecular Dynamics simulations for the same sphere sizes (dashed lines). The shapes of these density profiles are similar but for large spheres our model gives less structured water around the solute than the results of Ref. [18] – the oxygen peaks are sufficiently smaller.

3.4 *Nonlinear dielectric response of water to the field of ions*

Using RISM technique we calculated the screening factor $F(r) = \epsilon r \Phi(r)/q$ for a cation and anion of radius $a = 1.63$ Å (which corresponds to the Gourary–Adrian radius of Cl^- or Rb^+). We varied charges formally between $0.25e$ to $3.00e$, positive and negative-wise. The results are shown in Fig. 5 as contour maps on the distance/charge plain. The distances were measured from the ion surfaces.

In the linear response regime the profile of $F(r)$ must not depend upon the value of the charge. On the contrary, in Fig. 5 we see a substantial effect of the absolute value of charge on $F(r)$. This suggests

1 a 'specific' electrostriction: strong draw of water protons towards the anion and their repulsion from the
2 cation. The effect is asymmetric. Protons and the whole water molecules shift strongly towards the anion
3 at larger charges, whereas a cation cannot draw the oxygens of the first hydration shell considerably closer
4 than where they are in the 'linear response' case. This is seen in the ion-oxygen and ion-hydrogen RDF
5 maps shown in the same figure.
6
7
8
9

10 A more detailed comparison of the electrostatic field near anions and cations with different radii is shown
11 in Figs. 6 and 7. We see an essential ion size effect here. Namely, the hydration of a small anion (Fig. 6)
12 triggers strong overscreening in the first hydration shell caused by crowding of hydrogen near the surface
13 of the anion. The overscreening weakens with the increase of the radius of anion (Fig. 7).
14
15
16
17

18 The deficiency of the linear-response nonlocal electrostatic theory is demonstrated in Fig. 8 for monova-
19 lent cations and anions for two ionic radii: 1.0 \AA and 2.0 \AA . In this figure we compare the screening factors
20 $F(r)$ obtained with direct RISM calculations and the nonlocal theory with RISM bulk susceptibility and
21 Smearred Born Spheres model for the ion charge density (8) with decay parameter $\xi = 0 \text{ \AA}$ (dashed),
22 $\xi = 0.2 \text{ \AA}$ (dotted) and $\xi = 0.4 \text{ \AA}$ (dash-dotted). The direct RISM results show a discrepancy with the
23 linear response theory, particularly visible in the case of $\xi = 0 \text{ \AA}$ (which corresponds to the Born sphere
24 model, see (7)) and less pronounced for $\xi = 0.4 \text{ \AA}$. Note that in the case of anions there is no qualita-
25 tive difference in the character of the screening factors of the linear and 'nonlinear' theories, whereas for
26 cations the screening factors oscillate in counter-phase. Presumably, this is due to the impeded ability of
27 the solvent to 'overscreen' the charge of cation because of the limited ability of oxygen atoms to approach
28 the ion core.
29
30
31
32
33
34
35
36
37
38
39

40 4 Conclusions

41 Lessons from this study are as follows:
42
43
44

- 45 (i) The overscreening effect, if present in water, is usually substantially damped by the ion-induced per-
46 turbation of water structure in the vicinity of the ion. A conjecture in the past, this has now been
47 demonstrated by model calculations.
48
49
- 50 (ii) A huge overscreening resonance in the bulk response function does not prevent reproduction of the
51 observed free energies of hydration. Smearred by the distortions of water structure caused by the presence
52 of the ion, this effect is furthermore partially compensated by the short range van der Waals repulsion.
53
54
55
- 56 (iii) The electric field of an ion causes nonlinearity of water polarisation response. The effect manifests itself
57 differently at different distances, and is stronger for anions than for cations of comparable size.
58
59
60

- 1 (iv) Due to all these effects of perturbation of the structure of water by the ion, the linear response theory
2 may not be a good approximation, less for calculation of hydration free energies, and more for the
3 electric field distribution around the ion.
4
5
6
7 (v) The distribution of electric potential at distances of short-range structure of water, predicted by the
8 molecular theory, lies far from those given by the macroscopic Coulomb's law. Furthermore, even a
9 neutral hydrophobic sphere can be a source of electric field in water, which, however, vanishes beyond
10 short range structure scales.
11
12
13
14

15 These conclusions are sound, but they rest on an approximate statistical-mechanical description of a
16 crude model of water (rigid site-site interaction model). It is not clear, for instance, where the true border
17 for emergence of nonlinear effects lies: rigid vs soft models of water must not necessarily give the same
18 answer. All in all, these conclusions **must be** double-checked with better models, taking into account
19 a realistic charge distribution inside each water molecule. Future *ab initio* quantum molecular dynamic
20 simulations may have their final say.
21
22
23
24
25
26
27
28
29
30

31 5 Acknowledgments

32
33
34 MVF wishes to thank Prof. Gennady N. Chuev (Institute of Experimental and Theoretical Biophysics,
35 Russian Academy of Sciences, Pushchino) for helpful discussions of various aspects of Statistical Mechan-
36 ics and Integral Equations Theory. Some of the questions suggested in this article have been influenced
37 by discussions of AAK with Prof. Margarita N. Rodnikova (Kurnakov Institute of General and Inorganic
38 Chemistry, Russian Academy of Sciences, Moscow), Prof. George G. Malenkov (Institute of Physical Chem-
39 istry and Electrochemistry, Russian Academy of Sciences, Moscow), Prof. Philippe A. Bopp (University
40 of Bordeaux), and Dr Godehard Sutmann (Research Centre Juelich) in the past. This study was started
41 when MVF was a CSCB Research Fellow at the Centre for Synthesis and Chemical Biology, University
42 College Dublin. He acknowledges support provided by Dr Edward G. Timoshenko at the initial stage of
43 this work. AAK acknowledges Royal Society Wolfson Merit Research Award. Both authors are thankful to
44 Prof. Jean-Pierre Hansen (University of Cambridge), Dr Aaron Wynveen (Imperial College London) and
45 Dr Fernando Bresme (Imperial College London) for critical reading of the manuscript. Special thanks are
46 to Dr Joachim Dzubiella (University of California, San Diego) for providing numerical arrays of the MD
47 data published in [18].
48
49
50
51
52
53
54
55
56
57
58
59
60

Appendix A:

A.1 Modified SPC/E water model

In the SPC/E water model [41], the water molecules are assumed to be rigid with a fixed angle $\theta = 109.47^\circ$ between the two OH bonds. The intramolecular OH bond has the length $r_{OH} = 1.0 \text{ \AA}$. The non-bonded interactions between two water molecules are given by the sum of the site-site interaction potentials, u_{ij} :

$$u_{ij}(r) = \frac{q_i q_j}{r} + \frac{C_{ij}^{12}}{r^{12}} - \frac{C_{ij}^6}{r^6}, \quad (\text{A1})$$

where i and j represent O and H atoms. In the original SPC/E model $C_{OH}^6 = C_{OH}^{12} = 0$, therefore, there are only attractive electrostatic interactions between H and O atoms. Nevertheless, this model works very well for molecular simulations – hydrogen and oxygen atoms do not 'overlap' because of the strong repulsion between the oxygen atoms and rigid bonds in the SPC/E model. However, with such form of u_{OH} , numerical solutions of Eqns. (14) and (15) can become divergent [40, 71]. To eliminate this artifact, Lue and Blankshtein [40, 71] slightly modified the SPC parameters assuming a weak Lennard-Jones repulsive potential between the water oxygens and hydrogens. We use here the MSPC/E parameters from their work [40]: $C_{OH}^{12} = 34.69 \text{ eV} \cdot \text{\AA}^{12}$, $C_{OH}^6 = 0$. Other parameters were the same as in the original SPC/E model [41].

A.2 RISM with dielectric corrections.

For calculation of water RDFs we used a reformulation of the RISM theory with dielectric corrections [22, 72, 73]. In this method, the Coulomb part of the solvent-solvent interaction potential $q_i q_j / r_{ij}$ is rescaled as $A q_i q_j / r_{ij}$ to provide accurate screening of the long-range interactions. The renormalisation factor A is determined by the phenomenological dielectric constant ϵ and the averaged molecular dipole moment of water $\langle d_v^2 \rangle$ as:

$$A = \frac{1 + \epsilon(3y - 1)}{3y(\epsilon - 1)}; \quad y = \frac{4\pi\beta\rho_v\langle d_v^2 \rangle}{9}, \quad (\text{A2})$$

where ρ_v is the average solvent density. For the rigid water model used here, $\langle d_v^2 \rangle = d_v^2$. This, rather simple, approach makes use of the known asymptotic form of the correlation functions but, in general, more sophisticated techniques can be applied [98].

A.3 Treatment of the long-range solute-solvent interaction potential

The long-range character of the Coulomb potential causes some numerical artifacts in the treatment of electrostatic solute-solvent interactions. It is a common practice in numerical implementations of Integral Equations Theory to separate the direct correlation functions c_{ij} on short range c_{ij}^{SR} and long range $f_{ij}(r)$ parts in the following way [57, 99]:

$$c_{ij}^{SR}(r) = c_{ij}(r) + f_{ij}(r), \quad (\text{A3})$$

$$f_{ij}(r) = -\beta q_i q_j \operatorname{erf}(\alpha r)/r, \quad (\text{A4})$$

where q_i and q_j are the site charges, erf is the error function, and α is an appropriately chosen constant ($\alpha = 1 \text{ \AA}^{-1}$ in our calculations). The final results are independent from α , it influences only on the convergence of the algorithm. The function $f_{ij}(r)$ has an analytical representation in Fourier space which vanishes as k approaches zero:

$$f_{ij}(k) = -4\pi\beta q_i q_j \exp[-k^2/(4\alpha^2)]/k^2. \quad (\text{A5})$$

This fact makes it possible to treat separately the short-range and long-range parts of the electrostatic potential in the real (short-range part) and reciprocal (long-range part) spaces with use of the Fast Fourier Transform.

A.4 Procedure for MD Simulations

In this work we used the Gromacs MD software package [100,101]. For simulations of the bulk water solution we used 1716 SPC/E water molecules in an octahedral box with periodic boundary conditions. Electrostatic interactions were treated with use of the Particle Mesh Ewald (PME) summation technique [7]. The first step in the computational procedure was minimisation of the potential energy of the system by using a version of the steepest descent algorithm [100, 101]. Then we performed an equilibration run for one nanosecond with NVT conditions to equilibrate solvent molecules in the box. Afterwards we performed another 5.0 ns run for the following equilibration of the system with NPT ensemble where the pressure and the temperature were maintained at 1.0 atmosphere and 300.0 K by coupling the system to a heat bath via the Berendsen thermostat [102]. Such long preliminary simulations provided a good equilibration of the system. Then we performed a production run for 5.0 ns to collect the data. We collected the data

each 1.0 *ps*. For integration of the Newton's equations of motion we used the velocity Verlet algorithm with a timestep of 2.0 *fs*. For preprocessing and analysis of the MD data we used the GROMACS analysis tool [100, 101]. For further preprocessing of the obtained arrays of parameters we used the OCTAVE software [103].

References

- [1] O. Ia. Samoilov (Ed.). *Structure of aqueous electrolyte solutions and the hydration of ions*, Consultants Bureau, New York (1965).
- [2] B. E. Conway (Ed.). *Ionic Hydration in Chemistry and Biophysics*. Elsevier, Amsterdam (1981).
- [3] Y. Marcus. *Ion solvation*. John Wiley & Sons, Chichester, UK, (1985).
- [4] A. A. Kornyshev R. R. Dogonadze, E. Kalman and J. Ulstrup (Eds). *The Chemical Physics of Solvation. Part A*. Elsevier, Amsterdam (1985).
- [5] A. A. Kornyshev R. R. Dogonadze, E. Kalman and J. Ulstrup (Eds). *The Chemical Physics of Solvation. Part B*. Elsevier, Amsterdam (1986).
- [6] R. R. Dogonadze, E. Kalman, A. A. Kornyshev, and J. Ulstrup, (Eds). *The Chemical Physics of Solvation. Part C*. Elsevier, Amsterdam (1988).
- [7] P. R. Schleyer, (Ed.). *Encyclopedia of Computational Chemistry*. John Wiley & Sons, Chichester, UK (1998).
- [8] P. A. Bopp, A. A. Kornyshev, and G. Sutmann. *Phys. Rev. Lett.*, **76**, 1280 (1996).
- [9] G. Hummer, L. R. Pratt, and A. E. Garcia. *J. Phys. Chem. B*, **100**, 1206 (1996).
- [10] A. P. Lyubartsev and A. Laaksonen. *J. Phys. Chem. B*, **100**, 16410 (1996).
- [11] G. Hummer, L. R. Pratt, and A. E. Garcia. *J. Am. Chem. Soc.*, **119**, 8523 (1997).
- [12] R. M. Lynden-Bell and J. C. Rasaiah. *J. Chem. Phys.*, **107**, 1981 (1997).
- [13] P. A. Bopp, A. A. Kornyshev, and G. Sutmann. *J. Chem. Phys.*, **109**, 1939 (1998).
- [14] D. M. Huang, P. L. Geissler, and D. Chandler. *J. Phys. Chem. B*, **105**, 6704 (2001).
- [15] J. Dzubiella and J. P. Hansen. *J. Chem. Phys.*, **119**, 12049 (2003).
- [16] Y. Laudernet, T. Cartailier, P. Turq, and M. Ferrario. *J. Phys. Chem. B*, **107**, 2354 (2003).
- [17] M. V. Vener, I. V. Leontyev, and M. V. Basilevsky. *J. Chem. Phys.*, **119**, 8038 (2003).
- [18] J. Dzubiella and J. P. Hansen. *J. Chem. Phys.*, **121**, 5514, (2004).
- [19] D. Chandler. *J. Chem. Phys.*, **67**, 1113 (1977).
- [20] F. Hirata, B. M. Pettitt, and P. J. Rossky. *J. Chem. Phys.*, **77**, 509 (1982).
- [21] B. M. Pettitt and P. J. Rossky. *J. Chem. Phys.*, **77**, 1451 (1982).
- [22] B. M. Pettitt and P. J. Rossky. *J. Chem. Phys.*, **84**, 5836 (1986).
- [23] F. O. Raineri, H. Resat, and H. L. Friedman. *J. Chem. Phys.*, **96**, 3068 (1992).
- [24] S. H. Chong and F. Hirata. *J. Phys. Chem. B*, **101**, 3209 (1997).
- [25] F. Bresme. *J. Chem. Phys.*, **108**, 4505 (1998).
- [26] A. Kovalenko and T. N. Truong. *J. Chem. Phys.*, **113**, 7458 (2000).
- [27] R. R. Dogonadze and A. A. Kornyshev. *J. Chem. Soc., Faraday Trans.*, **70**, 1121, (1974).
- [28] A. A. Kornyshev. *J. Chem. Soc., Faraday Trans.*, **79**, 651, (1983).
- [29] A. A. Kornyshev. In *The Chemical Physics of Solvation. Part A*, R. R. Dogonadze, E. Kalman, A. A. Kornyshev, and J. Ulstrup (Eds), pp. 77, Elsevier, Amsterdam (1985).
- [30] A. A. Kornyshev and G. Sutmann. *J. Chem. Phys.*, **104**, 1524 (1996).
- [31] M. V. Basilevsky and D. F. Parsons. *J. Chem. Phys.*, **108**, 9107, (1998).
- [32] J. Liszi and I. Ruff. In *The Chemical Physics of Solvation. Part A*, R. R. Dogonadze, E. Kalman, A. A. Kornyshev, and J. Ulstrup (Eds), pp. 119, Elsevier, Amsterdam (1985).

- 1 [33] Y. Hatano, T. Kakitani, A. Yoshimori, M. Saito, and N. Mataga. *J. Phys. Soc. Jpn.*, **59**, 1104 (1990).
- 2 [34] A. A. Kornyshev and G. Sutmann. *Phys. Rev. Lett.*, **79**, 3435 (1997).
- 3 [35] A. A. Kornyshev and G. Sutmann. *J. Electroanal. Chem.*, **450**, 143, (1998).
- 4 [36] A. Geiger. *Ber. Bunsen-Ges. Phys. Chem*, **85**, 52 (1981).
- 5 [37] M. N. Buslaeva and O. Ya. Samoilov. In *The Chemical Physics of Solvation. Part A*, R. R. Dogonadze, E. Kalman, A. A. Kornyshev,
- 6 and J. Ulstrup (Eds), pp. 391, Elsevier, Amsterdam (1985).
- 7 [38] J-Y. Huot and C. Jolicoer. In *The Chemical Physics of Solvation. Part A*, R. R. Dogonadze, E. Kalman, A. A. Kornyshev, and
- 8 J. Ulstrup (Eds), pp. 417, Elsevier, Amsterdam (1985).
- 9 [39] D. Chandler and H. C. Andersen. *J. Chem. Phys.*, **57**, 1930 (1972).
- 10 [40] L. Lue and D. Blankschtein. *J. Phys. Chem. B*, **96**, 8582, (1992).
- 11 [41] H. J. C. Berendsen, J. R. Grigera, and T. P. Straatsma. *J. Phys. Chem. B*, **91**, 6269 (1987).
- 12 [42] A. A. Kornyshev and G. Sutmann. *J. Mol. Liq.*, **82**, 151 (1999).
- 13 [43] R. F. W. Bader and G. A. Jones. *Can. J. Chem.*, **41**, 586 (1963).
- 14 [44] D. Spangberg and K. Hermansson. *J. Chem. Phys.*, **120**, 4829 (2004).
- 15 [45] A. G. Donchev, V. D. Ozrin, M. V. Subbotin, O. V. Tarasov, and V. I. Tarasov. *Proc. Natl. Acad. Sci. U. S. A.*, **102**, 7829 (2005).
- 16 [46] J. W. Caldwell and P. A. Kollman. *J. Phys. Chem. B*, **99**, 6208 (1995).
- 17 [47] S. Walbran and A. A. Kornyshev. *J. Chem. Phys.*, **114**, 10039 (2001).
- 18 [48] E. Harder, J. D. Eaves, A. Tokmakoff, and B. J. Berne. *Proc. Natl. Acad. Sci. U. S. A.*, **102**, 11611 (2005).
- 19 [49] E. Spohr, P. Commer, and A. A. Kornyshev. *J. Phys. Chem. B*, **106**, 10560 (2002).
- 20 [50] A. A. Kornyshev, A. M. Kuznetsov, E. Spohr, and J. Ulstrup. *J. Phys. Chem. B*, **107**, 3351 (2003).
- 21 [51] J. VandeVondele, M. Krack, F. Mohamed, M. Parrinello, T. Chassaing, and J. Hutter. *Comput. Phys. Commun.*, **167**, 103 (2005).
- 22 [52] J. C. Grossman, E. Schwegler, E. W. Draeger, F. Gygi, and G. Galli. *J. Chem. Phys.*, **120**, 300 (2004).
- 23 [53] I. F. W. Kuo, C. J. Mundy, M. J. McGrath, J. I. Siepmann, J. VandeVondele, M. Sprik, J. Hutter, B. Chen, M. L. Klein, F. Mohamed,
- 24 M. Krack, and M. Parrinello. *J. Phys. Chem. B*, **108**, 12990 (2004).
- 25 [54] J. VandeVondele and M. Sprik. *Phys. Chem. Chem. Phys.*, **7**, 1363 (2005).
- 26 [55] P. A. Monson and G. P. Morriss. *Adv. Chem. Phys.*, **77**, 451 (1990).
- 27 [56] J.-P. Hansen and I. R. McDonald. *Theory of simple liquids*. Academic Press, London (1991).
- 28 [57] F. Hirata (Ed.). *Molecular theory of solvation*. Kluwer Academic Publishers, Dordrecht, Netherlands (2003).
- 29 [58] A. Kovalenko and F. Hirata. *J. Chem. Phys.*, **112**, 10403 (2000).
- 30 [59] H. A. Yu, B. M. Pettitt, and M. Karplus. *J. Am. Chem. Soc.*, **113**, 2425 (1991).
- 31 [60] T. Fonseca and B. M. Ladanyi. *J. Chem. Phys.*, **93**, 8148, (1990).
- 32 [61] C. Martin, M. Lombardero, M. Alvarez, and E. Lomba. *J. Chem. Phys.*, **102**, 2092 (1995).
- 33 [62] M. Kinoshita, Y. Okamoto, and F. Hirata. *J. Comput. Chem.*, **19**, 1724 (1998).
- 34 [63] R. Ramirez, M. Mareschal, and D. Borgis. *Chem. Phys.*, **319**, 261 (2005).
- 35 [64] T. Imai, M. Kinoshita, and F. Hirata. *Bull. Chem. Soc. Jpn.*, **73**, 1113 (2000).
- 36 [65] D. Chandler, J. D. McCoy, and S. J. Singer. *J. Chem. Phys.*, **85**, 5977 (1986).
- 37 [66] A. Kovalenko and F. Hirata. *J. Phys. Chem. B*, **103**, 7942 (1999).
- 38 [67] A. Kovalenko and F. Hirata. *J. Chem. Phys.*, **110**, 10095 (1999).
- 39 [68] L. Blum and A. J. Torruella. *J. Chem. Phys.*, **56**, 303 (1972).
- 40 [69] C. M. Cortis, P. J. Rossky, and R. A. Friesner. *J. Chem. Phys.*, **107**, 6400 (1997).
- 41 [70] G. N. Chuev, S. Chiodo, S. E. Erofeeva, M. V. Fedorov, N. Russo, and E. Sicilia. *Chem. Phys. Lett.*, **418**, 485 (2006).
- 42 [71] L. Lue and D. Blankschtein. *J. Chem. Phys.*, **102**, 5427 (1995).
- 43 [72] P. T. Cummings and G. Stell. *Mol. Phys.*, **44**, 529 (1981).
- 44 [73] P. J. Rossky, B. M. Pettitt, and G. Stell. *Mol. Phys.*, **50**, 1263 (1983).
- 45 [74] A. A. Kornyshev. *Electrochim. Acta*, **26**, 1 (1981).
- 46
- 47
- 48
- 49
- 50
- 51
- 52
- 53
- 54
- 55
- 56
- 57
- 58
- 59
- 60

- 1 [75] S. J. Singer and D. Chandler. *Mol. Phys.*, **55**, 621 (1985).
- 2 [76] J. G. Kirkwood. *J. Chem. Phys.*, **3**, 300 (1935).
- 3 [77] Q. H. Du, D. Beglov, and B. Roux. *J. Phys. Chem. B*, **104**, 796 (2000).
- 4 [78] A. Kovalenko and F. Hirata. *J. Chem. Phys.*, **113**, 2793 (2000).
- 5 [79] S. Chiodo, G. N. Chuev, S. E. Erofeeva, M. V. Fedorov, N. Russo, and E. Sicilia. *Int. J. Quantum Chem.*, in press, (2006).
- 6 [80] G. N. Chuev and M. V. Fedorov. *J. Chem. Phys.*, **120**, 1191, (2004).
- 7 [81] G. N. Chuev and M. V. Fedorov. *J. Comput. Chem.*, **25**, 1369, 2004.
- 8 [82] M. V. Fedorov and G. N. Chuev. *J. Mol. Liq.*, **120**, 159 (2005).
- 9 [83] M. S. Skaf. *THEOCHEM*, **505**, 45 (2000).
- 10 [84] P. Bopp, G. Jancso, and K. Heinzinger. *Chem. Phys. Lett.*, **98**, 129 (1983).
- 11 [85] A. D. Trokhymchuk, M. F. Holovko, and K. Heinzinger. *J. Chem. Phys.*, **99**, 2964 (1993).
- 12 [86] A. A. Kornyshev, D. A. Kossakowski, and M. A. Vorotyntsev. In *Condensed Matter Physics Aspects of Electrochemistry*, M. P. Tosi and A. A. Kornyshev (Eds.), pp. 92, World Scientific, Singapore (1991).
- 13 [87] A. Ben-Naim and Y. Marcus. *J. Chem. Phys.*, **81**, 2016 (1984).
- 14 [88] M. Born. *Z. Phys.*, **1**, 45 (1920).
- 15 [89] B. S. Gourary and F. J. Adrian. In *Solid State Physics-Advances in Research and Applications*, F. Seitz, D. Turnbull, and H. Ehrenreich (Eds), **10**, pp. 127–247, Academic Press, New York (1960).
- 16 [90] M. Salomon. *J. Phys. Chem. B*, **74**, 2519 (1970).
- 17 [91] J. E. B. Randles. *Trans. Faraday Soc.*, **52**, 1573 (1956).
- 18 [92] W. R. Fawcett. *J. Phys. Chem. B*, **103**, 11181 (1999).
- 19 [93] R. Ramirez, R. Gebauer, M. Mareschal, and D. Borgis. *Phys. Rev. E*, **66**, 031206 (2002).
- 20 [94] G. Hummer, S. Garde, A. E. Garcia, M. E. Paulaitis, and L. R. Pratt. *J. Phys. Chem. B*, **102**, 10469 (1998).
- 21 [95] P. Jedlovsky, M. Předota, and I. Nezbeda. *Mol. Phys.*, **104**, 2465, 2006.
- 22 [96] K. Tay and F. Bresme. Unpublished results, (2006).
- 23 [97] S. I. Mamatkulov, P. K. Khabibullaev, and R. R. Netz. *Langmuir*, **20**, 4756 (2004).
- 24 [98] F. O. Raineri and G. Stell. *J. Phys. Chem. B*, **105**, 11880 (2001).
- 25 [99] K. C. Ng. *The J. Chem. Phys.*, **61**, 2680 (1974).
- 26 [100] H. J. C. Berendsen, D. van der Spoel, and R. van Drunen. *Comput. Phys. Commun.*, **91**, 43 (1995).
- 27 [101] E. Lindahl, B. Hess, and D. van der Spoel. *J. Mol. Model.*, **7**, 306 (2001).
- 28 [102] H. J. C. Berendsen, J. P. M. Postma, W. F. van Gunsteren, A. Dinola, and J. R. Haak. Molecular-dynamics with coupling to an external bath. *J. Chem. Phys.*, **81**, 3684 (1984).
- 29 [103] www.octave.org.
- 30 [104] Y. Marcus. *J. Chem. Soc., Faraday Trans.*, **83**, 2985 (1987).
- 31
- 32
- 33
- 34
- 35
- 36
- 37
- 38
- 39
- 40
- 41
- 42
- 43
- 44
- 45
- 46
- 47
- 48
- 49
- 50
- 51
- 52
- 53
- 54
- 55
- 56
- 57
- 58
- 59
- 60

Figure Captions

Figure 1. Longitudinal dielectric susceptibility $\chi(k)$ for the bulk MSPC/E water calculated with DRISM method (solid line) and for the bulk SPC/E water calculated with MD simulations (dashed line with circles). The graph reveals an exaggerated main 'overscreening'-resonance, exaggerated in the rigid site-site interaction molecule model, and the absence of Lorentzian decrease at small k (possibly also a consequence of this model).

Figure 2. Free energy of a neutral sphere, ΔG , versus sphere radius, a . This figure shows RISM values of ΔG (solid line) and analogous data (dashed line) from MD simulations [18].

Figure 3. Free energy of single ion hydration, ΔG , versus ion radius, a . The positions of the alkali-halide ions are marked by the corresponding Gourary and Adrian radii [89,92,104]. Symbols show experimental data for alkali cations and halide anions taken from different sources: \circ [Salomon [90]], \triangle [Randles [91]], and \square [Fawcett [92]]. Empty and filled symbols correspond to the cations and anions, respectively.

top) Solid line - RISM theory for cations; Dashed line - RISM theory for anions; Dash-dotted line - the classical Born's model [88];

bottom) The nonlocal theory data on ΔG with Smearred Born Sphere model of ion (8)- calculation via the Dogonadze-Kornyshev equation (9) with the RISM values of the longitudinal bulk dielectric susceptibility $\chi(k)$ (Fig. 1); Different lines correspond to different values of decay parameter ξ : dash-dotted line - $\xi = 0 \text{ \AA}$ (Born Sphere, see (7)) dashed and solid lines correspond to $\xi = 0.2 \text{ \AA}$ and $\xi = 0.4 \text{ \AA}$, respectively.

Figure 4. Electrostatic potential around an uncharged soft hydrophobic sphere immersed in MSPC/E water, shown for different radii of the sphere, as indicated. Somewhat closer position to the sphere of the water protons in the first hydration shell is sufficient to provide substantial nonzero fields that will decay at the scales of the short range order in water, the effect smaller for smaller spheres. The inset shows RISM values (solid line) of water oxygen (top) and hydrogen (bottom) density profiles around the spheres of two different sizes: $a = 1.0 \text{ \AA}$ and $a = 5.0 \text{ \AA}$ together with analogous data from MD simulations (dashed line) [18]

Figure 5. Nonlinear dielectric response of water to the field of ions - RISM calculations. Contour maps for (a) the screening factor $F(r) = \epsilon r \Phi(r)/q$, which should not depend on the charge if the linear response

was valid; **(b)** ion-oxygen RDF; and **(c)** ion-hydrogen RDF, calculated for a cation and anion (of radius $a = 1.63 \text{ \AA}$) - shown on the charge (q) - distance from the ion plane. The nonlinear effect is manifested in the change of the colourng of the vertical axis. The arrows show the regions of screening factors approaching the limit of macroscopic dielectric Response $F(r) \approx 1$. All data are represented as functions of the distance from the surface of the sphere, $r - a$

Figure 6. Visualisation of the **(a)** electrostatic potential, **(b)** screening factor and **(c)** ion-hydrogen (dashed line) and ion-oxygen (solid line) RDF, created by a singly charge anion/ cation (of radii $a = 1.0 \text{ \AA}$) as functions of the distance from the surface of the sphere, $r - a$: RISM results.

Figure 7. The same as Fig. 5 for $a = 2.0 \text{ \AA}$.

Figure 8. The discrepancy between the nonlocal linear response theory operating with the RISM bulk response function, and the direct RISM theory for singly charge cations (left) and anions (right). We use here two different radii of the sphere: $a = 1.0 \text{ \AA}$ (top) and $a = 2.0 \text{ \AA}$ (bottom). Different lines correspond to different values of decay parameter ξ : dashed line - $\xi = 0 \text{ \AA}$ (Born Sphere, see (7)) dotted and dash-dotted lines correspond to $\xi = 0.2 \text{ \AA}$ and $\xi = 0.4 \text{ \AA}$, respectively. Solid lines correspond to the direct IE results.

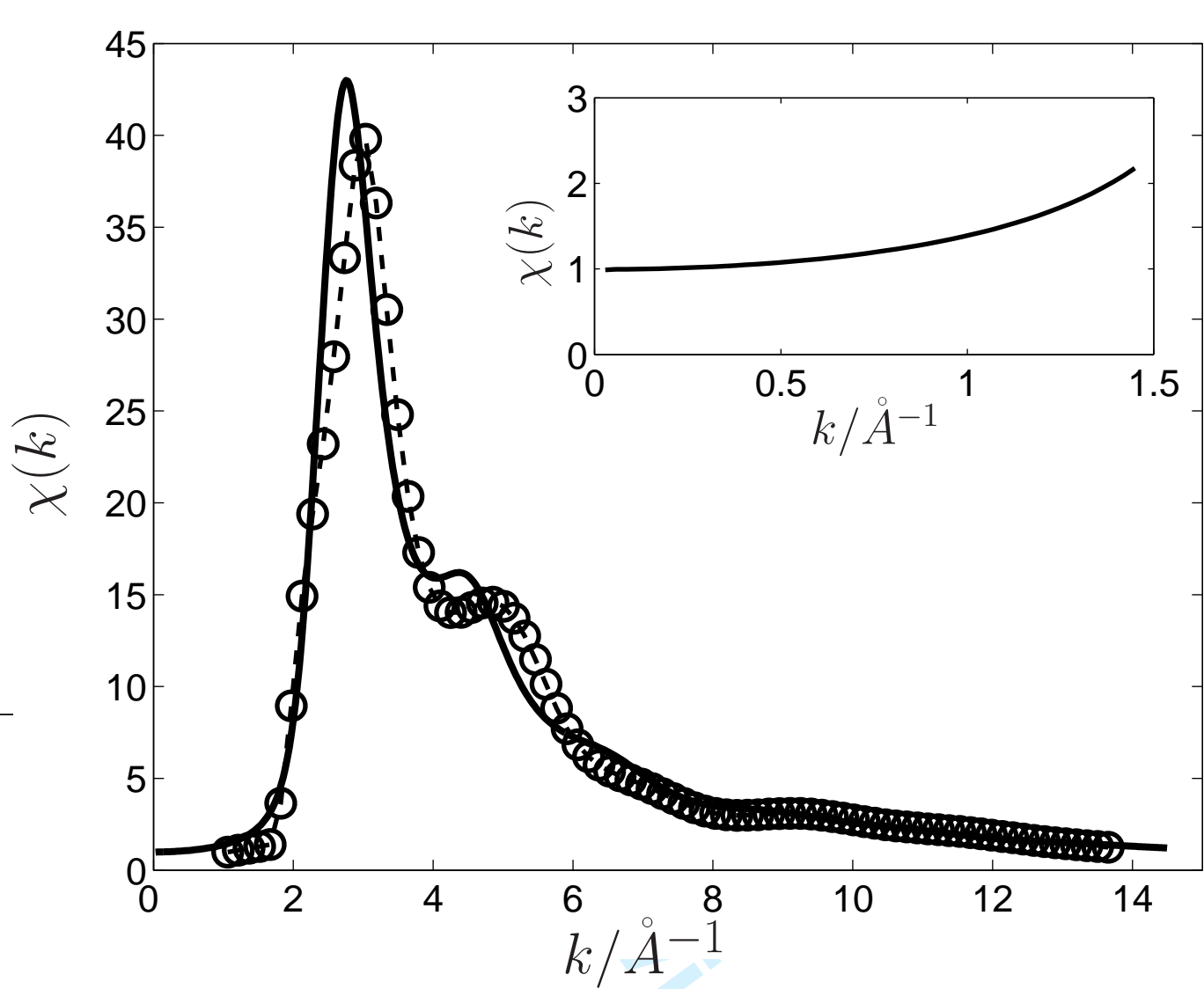


Figure 1.

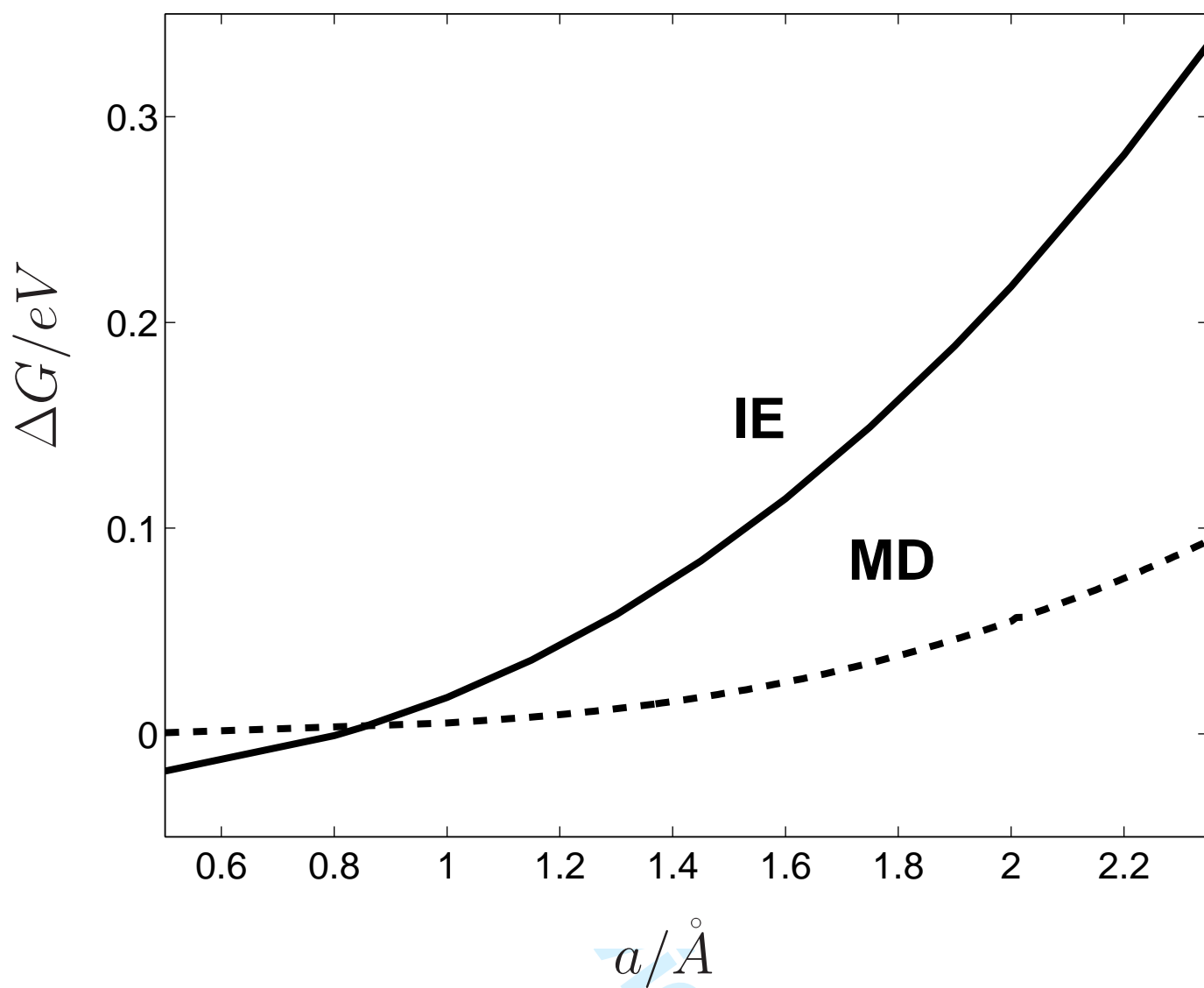


Figure 2.

1
2
3
4
5
6
7
8
9
10
11
12
13
14
15
16
17
18
19
20
21
22
23
24
25
26
27
28
29
30
31
32
33
34
35
36
37
38
39
40
41
42
43
44
45
46
47
48
49
50
51
52
53
54
55
56
57
58
59
60

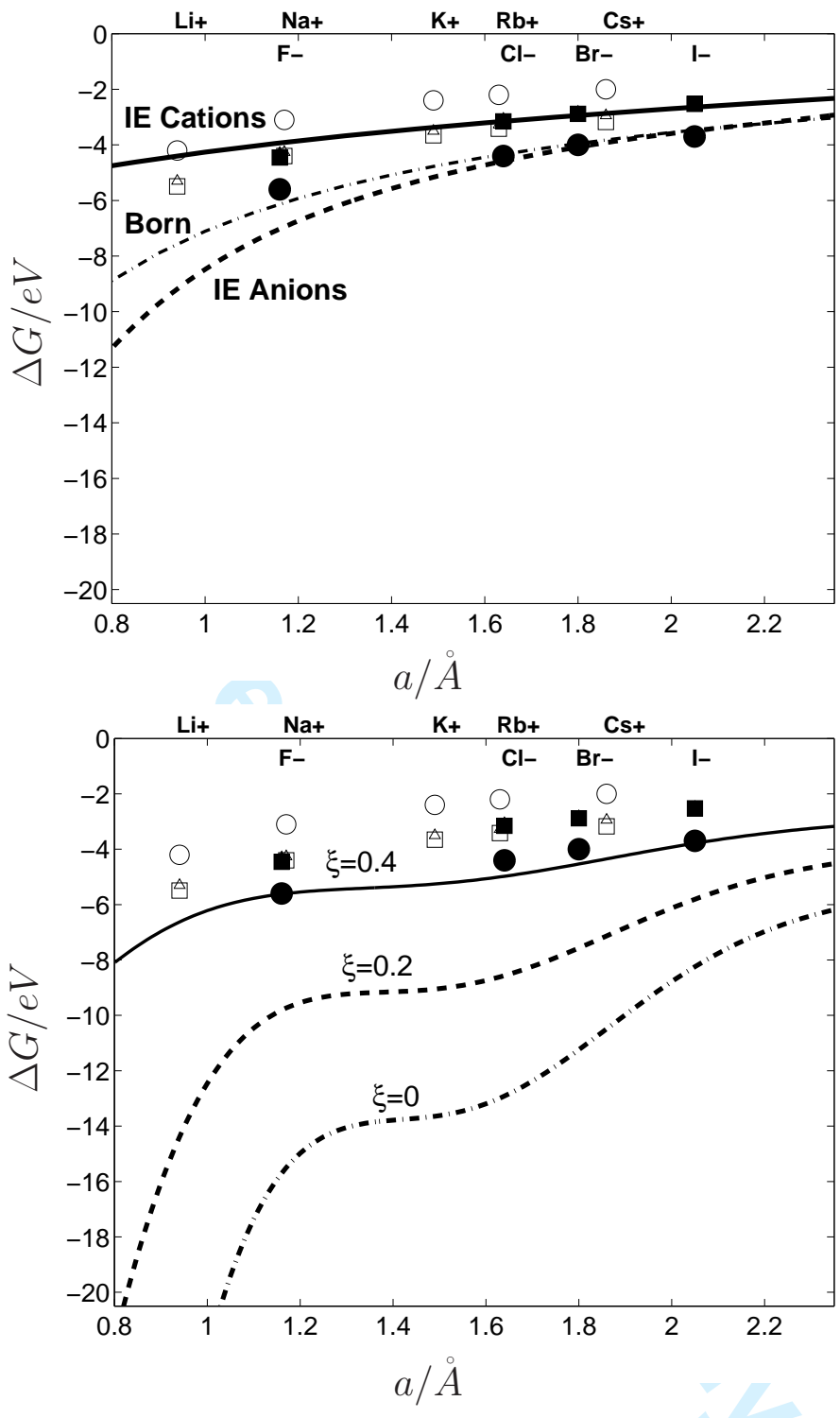


Figure 3.

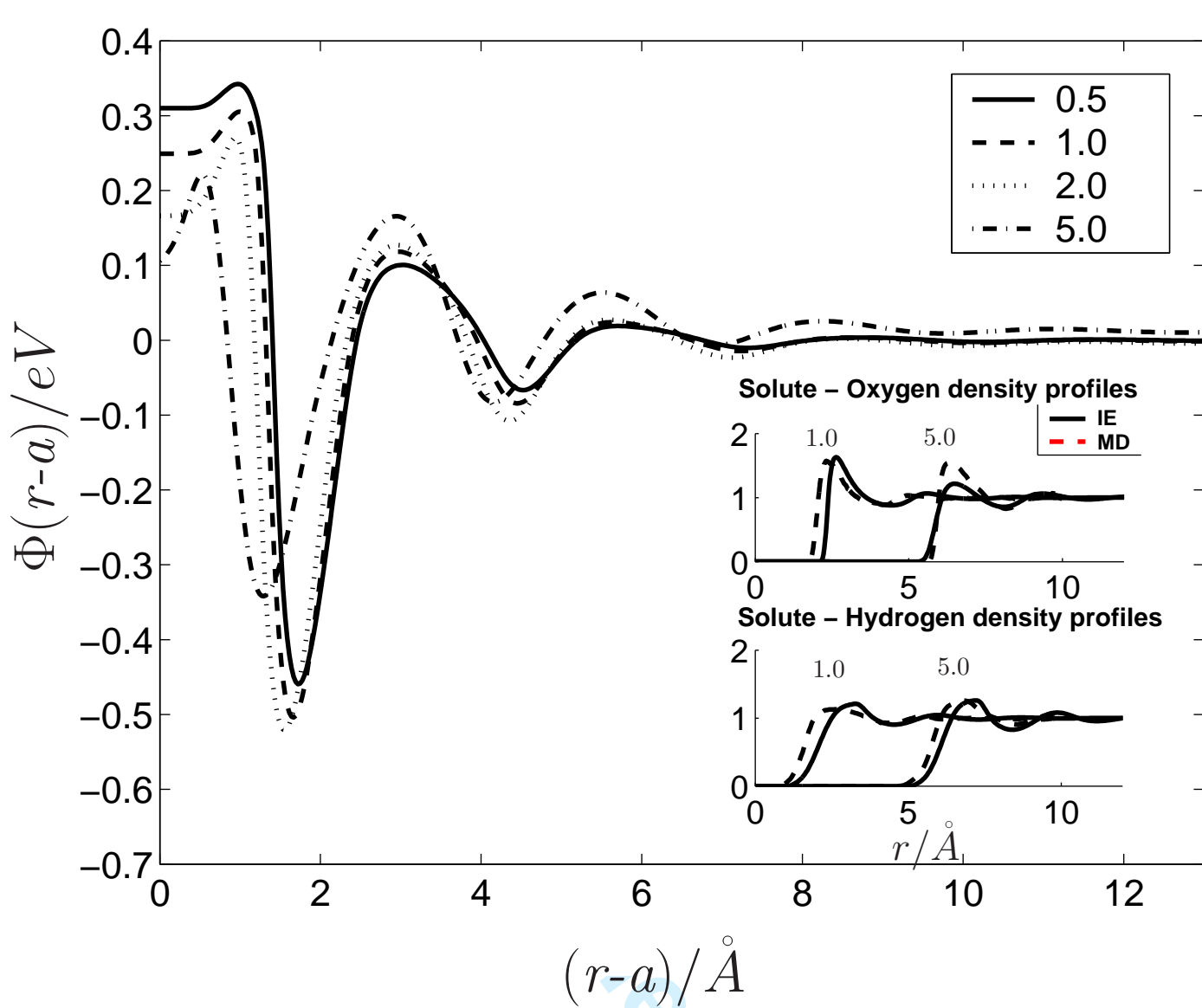


Figure 4.

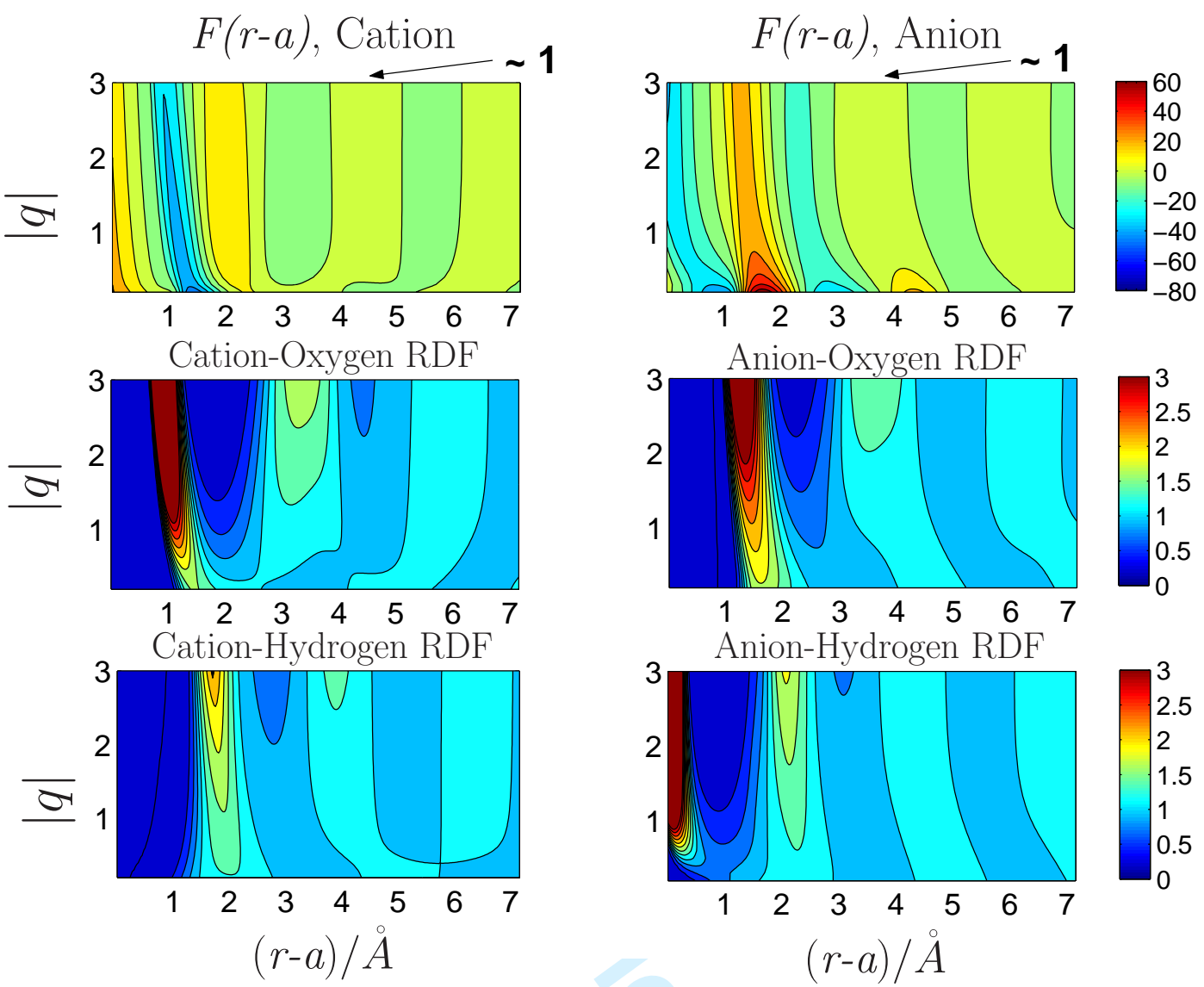


Figure 5.

new Only

1
2
3
4
5
6
7
8
9
10
11
12
13
14
15
16
17
18
19
20
21
22
23
24
25
26
27
28
29
30
31
32
33
34
35
36
37
38
39
40
41
42
43
44
45
46
47
48
49
50
51
52
53
54
55
56
57
58
59
60

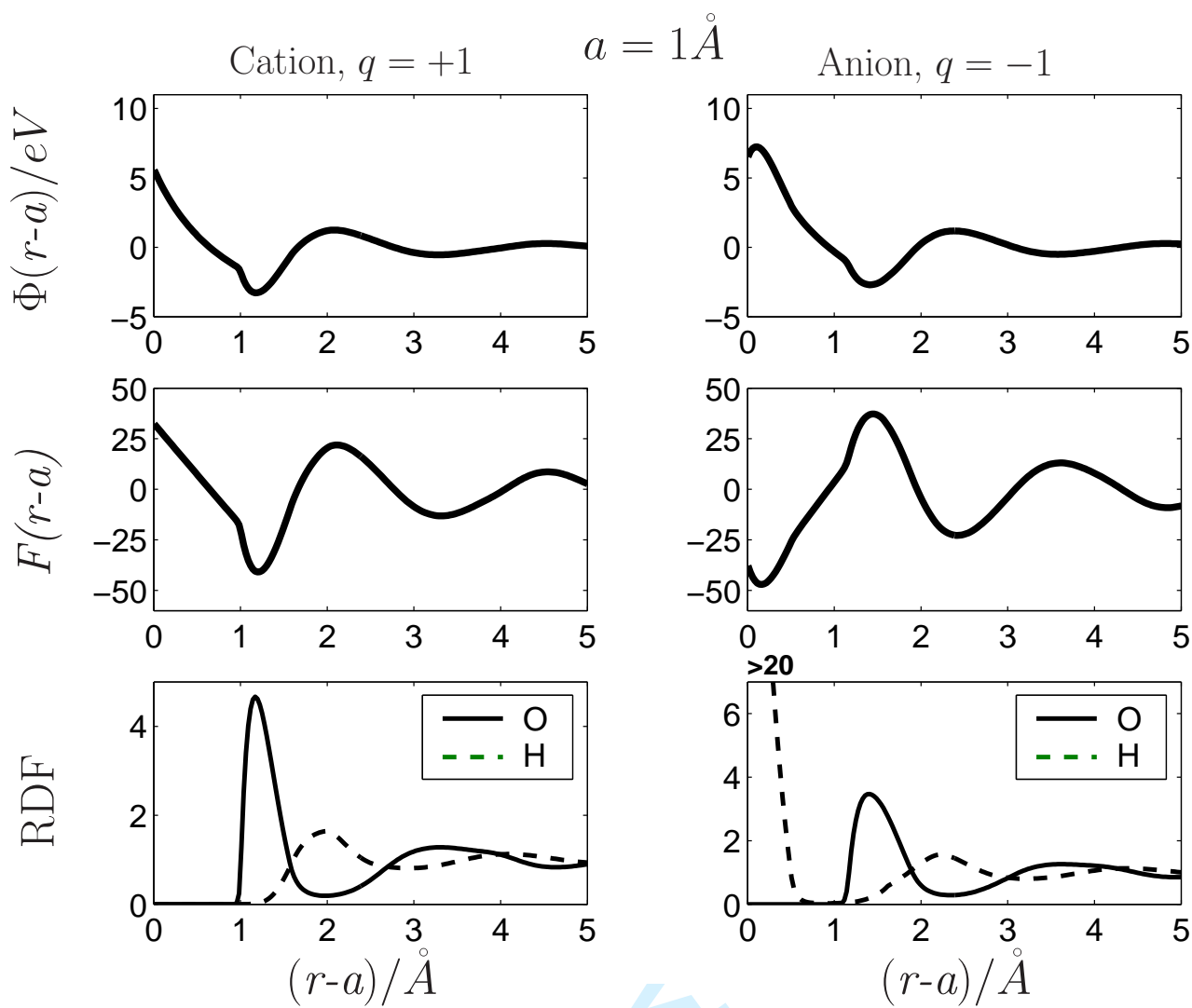


Figure 6.

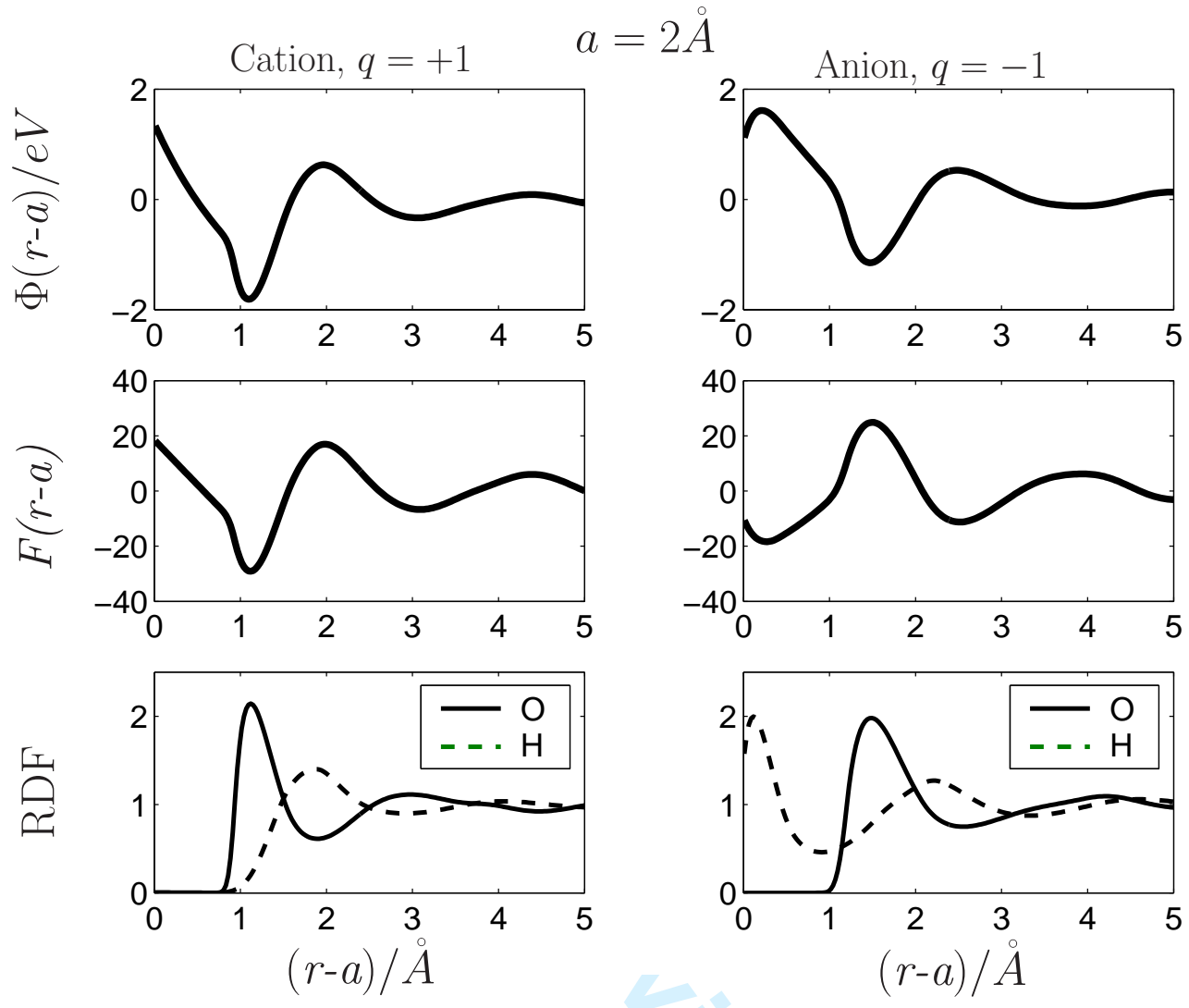


Figure 7.

view Only

